Chem. Chem. Technol., 2024,
Vol. 18, No. 4, pp. 524–534

Chemistry

POROUS SODIUM ALGINATE HYDROGEL FILMS FOR IMMEDIATE RELEASE DRUG DELIVERY SYSTEMS

Alina Sikach[1,✉], Halyna Bubela[1], Viktoriia Konovalova[1], Iryna Kolesnyk[1]

https://doi.org/10.23939/chcht18.04.524

Abstract. This study focuses on creating a method to produce ion-crosslinked alginate-based hydrogel systems that enable immediate drug release. The research investigates the kinetics of releasing a bactericidal drug to facilitate the healing process relief. The technique involves enhancing the immobilization of amphiphilic medicines on calcite microparticles, followed by concentrating them in the pores formed through a microparticle decomposition.

Keywords: alginate hydrogels, polysaccharide films, calcium carbonate microparticles, drug delivery system, ethonium, ion crosslinking.

1. Introduction

Recently, researchers have driven significant progress in the field of innovative targeted drug delivery systems aimed at increasing therapeutic efficacy while minimizing side effects and facilitating application.[1–5] A variety of controlled-release drug delivery systems with many advantages (*e.g.*, reduction of side effects, frequency of application, achievement of desired drug release profile) have already been developed.[6–10]

Hydrogel-based controlled-release transdermal drug delivery systems have received great attention owing to their non-invasive nature and ability to provide the desired drug release profile.[7,11,12] Hydrogels are three-dimensional (3D) water-swellable cross-linked hydrophilic networks, insoluble in water and biological fluids and capable of retaining moisture.[13–15] The significant water content helps to mimic the tissue's natural environment and hydrate dry wounds, promoting autolytic healing and maintaining a moist, heat-insulated wound bottom environment.[16] The hydration process in hydrogels is activated by hydrophilic functional groups (hydroxyl, amino, and carboxyl) in the polymer chains.[17–19] Furthermore, hydrogels can increase granulation and epithelization, reduce the temperature of the wound bottom, and minimize inflammation in the adjacent tissue.[20,21] However, compared with occlusive dressings hydrogels have many disadvantages (*e.g.*, high water concentration, unable to absorb significant amounts of wound exudate), making them unsuitable for bleeding wounds).[22] Swelling degree is one of the important parameters to study and control in hydrogel-based targeted drug delivery systems due to the maceration of healthy skin; thus, the skin around open wounds must be protected from excessive moisture.[23]

Hydrogels can be loaded with drugs of local or antibacterial action.[24–26] In addition, hydrogels provide oxygen and moisture vapor transport; however, the permeability to bacteria and liquids depends on the fabrication method and pore size. The porous mesh structure is also a requirement for the efficient loading of drugs into the polymer matrix and controlled release of biologically active agents;[27] furthermore, the limited swelling ability imparts easy removal of non-crosslinked polymers and non-immobilized drugs.[28]

Many biocompatible natural and synthetic polymers are used to create hydrogel wound dressings, such as poly(vinyl alcohol), poly(2-hydroxyethyl methacrylate), poly(N-isopropyl-2-acrylamide), chitosan, hyaluronic acid, gelatin, and sodium alginate.[29–31] Sodium alginate is now widely utilized in wound healing/treatment because of its excellent biocompatibility, ability to maintain a physiologically moist environment, good liquid absorption ability, and appealing anti-bacterial properties.[32–35] The stability of alginate gels, cross-linked by bivalent ions, provides the possibility to form hydrogels with targeted parameters and properties using various methods of adding ions to the reaction mixture. However, the harsh medium of polymer network formation (using crosslinking agents, radiating crosslinking, photo, and thermal crosslinking) remains an obstacle to the effective immobilization of drugs in the process of hydrogel fabrication for subsequent controlled release.[36]

The development of a technique for porous hydrogel fabrication capable of immobilizing drugs in the process of crosslinking polymer matrix should solve this

[1] Department of Chemistry, National University of Kyiv-Mohyla Academy, 2 Skovoroda St., Kyiv 04070, Ukraine
✉ *a.sikatch@ukma.edu.ua*

problem and allow to create the drug delivery system with immediate release controlled by the diffusion of a solvent or biological fluids. Wang *et al.*[37] templated alginate hydrogels on mesoporous valerite ($CaCO_3$) crystals. Ibuprofen[37] and bovine serum albumin (BSA)[38] were used as model drugs. In this study, valerite crystals with immobilized drugs were previously obtained. The crystal suspension was mixed with an alginate solution with subsequent cross-linking owing to the hydrolysis of glucono-δ-lactone. Acidification caused easy dissolution of $CaCO_3$ and release of Ca^{2+} *via* acidification crosslinked alginate for hydrogel formation. Macro-sized pores were formed as a result of the dissolution of calcium carbonate in the places where the valerite crystals were initially located. Ibuprofen[37] and BSA[38] were rapidly released from the samples, which confirmed the possibility of using $CaCO_3$ crystals as soluble cores for hydrogel crosslinking. The described method is multi-stage, in particular, the long procedure of multilayer coating of microparticles leads to additional material and time losses.

Surfactants, which are gemini quaternary ammonium salts, are widely used in medicine as antibacterial drugs.[39,40] The mechanism of action of quaternary ammonium salts as surface-active substances with an antibacterial effect has already been studied and consists in their absorption on the bacterial membrane and its destruction, which is associated with the negative charge of the bacterial membranes.[40,41] The positive charge of the surface-active substance promotes its absorption on the surface of bacteria and increases the antibacterial activity of the agent.[42,43] Surfactants as antibacterial drugs are on the market, for example, dequalinium chloride and ethonium. Ethonium is an antiseptic, disinfectant drug with antibacterial and fungicidal action, which has several positive effects, such as a calming effect, inhibition of the inflammatory process, and low toxicity.[40,44] The fungicidal activity of ethonium and its homologues was investigated by Oblak and his co-workers, who showed that most of the active molecules have an ethylenediamine spacer group and a decyl radical in the ether group, similar to the ethonium molecule.[40,45]

Herein, the method of porous hydrogel formation was improved by using another polymorphic modification of $CaCO_3$ (calcite) and ethonium[44] as a model antibacterial drug with the aim of ion-crosslinked hydrogel systems fabrication capable of immediate drug release. The kinetics of ethonium release for the healing process of open wounds was investigated. According to the proposed method, calcite microparticles (MPs) were directly mixed with the drug solution, making the process easier and reducing time and reagent losses. Hydrochloric acid was used to initiate the decomposition of microparticles and the formation of crosslinking Ca^{2+} ions *in situ*. The use of calcite microparticles and amphiphilic molecules of the drug allows the ethonium concentration on the surface of the MPs. Therefore, the drug release depends only on the hydrogel kinetics of swelling owing to the localization of the drug in the pores. As a result, a drug delivery system was developed with immediate drug release, increased bioavailability,[46,47] and reduced time of therapeutic effect onset.[48]

2. Experimental

2.1. Materials

Low molecular weight sodium alginate (NaAlg) with molecular weight of 250 kDa, Sigma-Aldrich), N,N-bis(carboxymethyl)-N,N,N',N'-tetramethylethylenediammonium chloride (ethonium) with pharmacopoeial purity (experimental production of the Institute of Organic Chemistry of the National Academy of Sciences of Ukraine) were used for hydrogel films formation. Anhydrous calcium chloride and sodium carbonate (Sigma-Aldrich) were utilized for calcium carbonate microparticles (MPs) synthesis. A 96 wt. % ethanol solution (UkrSpirt LLC) was used for $CaCO_3$ MPs purification. 0.1 M hydrochloric acid solution was used for $CaCO_3$ MPs decomposition.

2.2. Synthesis of Calcium Carbonate Microparticles

Microparticles of calcium carbonate for alginate crosslinking were synthesized by the method of an ion exchange reaction of salts according to the reaction:

$$CaCl_2 + Na_2CO_3 = CaCO_3\downarrow + 2NaCl \quad (1)$$

Solutions of sodium carbonate and calcium chloride with concentrations of 0.5 M were mixed with a stirring rate of 13,500 rpm. After one minute, the stirring was stopped, and the reaction mixture was left to settle for 10 min. The resulting precipitate was separated using filter paper and washed three times with 20 mL of distilled water. Final washing was carried out with 20 mL of 96% ethanol solution. After that, the microparticles were dried in an oven at a temperature of 50 °C for 72 hours.

2.3. Methods of Calcite Microparticles Characterization

The X-ray diffractometer (Philips X'Pert equipped with an X'Celerator Scientific detector, "Philips", the Netherlands) was utilized to confirm the polymorphic modification of the synthesized microparticles of calcium carbonate.

A transmission electron microscope (Tecnai F20 X-Twin, “FEI Europe B.V., P.O.”, The Netherlands) was

used to study the size and purity of the synthesized microparticles of calcium carbonate.

The study of ethonium adsorption by synthesized microparticles of calcium carbonate was carried out under static conditions. 100 mg of $CaCO_3$ was added to ethonium solutions with a concentration of 1-5 mg/mL. The resulting mixtures were stirred for 2 h at room temperature. After that, the mixture was kept for 24 h to establish equilibrium conditions. The concentration of ethonium was determined by the photocolorimetric method[49] using a bromocresol green indicator at a wavelength of 630 nm.

2.4. Modification of Sodium Alginate

NaAlg was modified with octan-1-amine (AlgM)[50] to obtain a partly hydrophobized polysaccharide (Fig. 1) capable of forming hydrophobic-hydrophobic bonds between octan-1-amine chains and carbon chains of amphiphilic active pharmaceutical ingredients. Sodium alginate 0.5 wt. % solution was converted into alginic acid solution by pH shift to 3.2 using 0.1 M HCl. Then, 200 mg 1-ethyl-3-(3-dimethyl aminopropyl) carbodiimide hydrochloride (EDCl) was added to the solution as an activator. 10 min later, octan-1-amine was added to the reaction mixture respectively in a ratio of 1:200. The resulting mixture was thermostated for 24 hours at 60 °C. AlgM was isolated from the reaction mixture through two successive filtrations: filter paper to isolate the activator and ultrafiltration using PM UP020 membrane. Ultrafiltration was used to separate AlgM after precipitation according to the addition of non-solvent (96% ethanol) to the first filtrate in a 4:1 ratio.

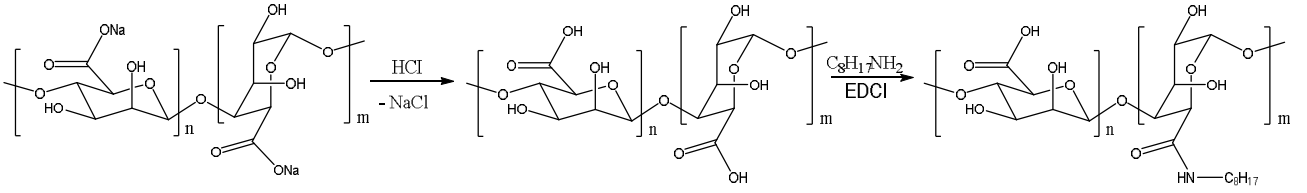

Fig. 1. Scheme of Na-Alg modification

2.5. Formation of Alginate Films

Alginate films (CaAlg and CaAlgM) were formed to study the influence of alginate modification on the swelling degree. The preparation of CaAlg and CaAlgM samples was conducted by the following procedure. 100 mg of calcium carbonate microparticles was added to 10 mL of a 4% solution of sodium alginate (NaAlg) or alginate modified with octan-1-amine (NaAlgM). The mixture was dispersed in an ultrasonic bath for 10 minutes. The final volume was poured into a Petri dish with a diameter of 75 mm and dried at a temperature of 50 °C f or 24 hours. Next, the dried sample is cooled to room temperature. After that, the film was placed in 20 mL of 0.1 M hydrochloric acid solution for 30 minutes with the aim of cross-linking.

Cross-linking of the samples occurred *via* the reaction between alginate and Ca^{2+} ions (Fig.2) which were released during the decomposition of calcium carbonate microparticles with hydrochloric acid (reaction 2). After cross-linking, the samples were washed 3 times with distilled water (20 mL) and dried for 24 h at 50°C.

$$CaCO_3 + 2HCl = CaCl_2 + CO_2\uparrow + H_2O; \quad (2)$$
$$CaCl_2 = Ca^{2+} + 2Cl^-$$

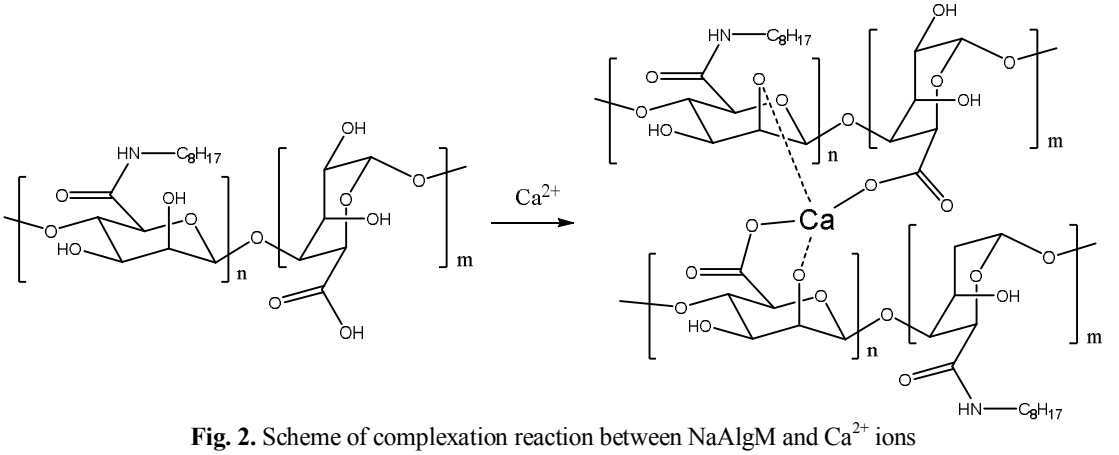

Fig. 2. Scheme of complexation reaction between NaAlgM and Ca^{2+} ions

2.6. Methods of Alginate Films Characterization

The kinetics and swelling degree were determined using a gravimetric method during 90 minutes at 20°C. Before measurements, the samples were placed in a desiccator for cooling to 20°C for 24 hours.

To study the pH dependence of the swelling solutions with pH 5.5 (corresponding to pH of healthy undamaged skin), pH 7.2 (coinciding to pH of inflammatory wounds), and pH 8.2 (correlating to pH of chronic wounds) were used.[44,51] The masses of the samples were determined every 10 minutes. Degrees of swelling (α) were calculated according to the following equation:

$$\alpha = \frac{m - m_0}{m_0} \cdot 100\ \%,$$

where m_o is the initial mass of a dry hydrogel film, and m is the mass of a swollen wet film at the moment of time.

The morphology and the surface of the cross-linked hydrogel samples were studied using an electron microscope (model 1430 VP, "LEO Ltd", Great Britain).

2.7. Formation of Alginate Films Loaded with Ethonium

Films with an immobilized bactericidal drug (Ca-Alg+Eth and Ca-AlgM+Eth) were formed according to the following method. 100 mg of $CaCO_3$ microparticles and 5 mL of ethonium solution with a concentration of 20 mg/mL were added to 5 mL of 4 wt. % solutions of NaAlg or NaAlgM and placed in an ultrasonic bath for 20 min. The final volume was put into a Petri dish with a diameter of 75 mm and dried at a temperature of 50 °C for 24 hours. The dried films were cooled to room temperature in a desiccator before cross-linking. Afterward, the samples were immersed in 20mL of 0.1 M hydrochloric acid solution and kept for 30 min. All the hydrogel films were washed 3 times with distilled water (20 mL) and dried for 24 h at 50°C.

2.8. Methods of Alginate Films Loaded with Ethonium Characterization

The surface area of the samples, the total pore volume, and the average pore size were determined by the method of nitrogen adsorption-desorption at a temperature of 77.4 K using the automatic gas sorption system Autosorb iQ and AsiQwin ("Quantachrome Instruments", USA). Samples were pre-prepared by degassing at 150 °C for 20 hours in a nitrogen atmosphere.

The evaluation of the kinetics of the drug release was performed at different pH and temperature values. The pH dependence of ethonium release was evaluated using solutions with different pH (pH 5.5, pH 7.2, and pH 8.2) as a swelling ratio determination. An evaluation of release was carried out with a stirring rate of 500 rpm and a temperature of 20°C (room temperature) or 37°C (physiological temperature). Ethonium concentrations were measured using a UV-1200 spectrophotometer at the wavelength of 220 nm every 10 min for 4 hours. Each sample measurement was conducted 3 times. All results were within 3% standard deviation;

$$Standard\ Deviation = \sqrt{\frac{\sum_{i=1}^{n}(x_i - \bar{x})^2}{n-1}}$$

where x_i is the value of the i^{th} point in the data set, $\bar{x}$ is the mean value of the data set, n is the number of data points in the data set

The drug release usually occurs as a first-order reaction according to the laws of chemical kinetics. Regarding the kinetic modeling, data for the ethonium release were fitted to the first-order reaction; thus, to determine the rate constants plots were constructed in the coordinates of the linear form of the first-order release kinetics:[52]

$$kt = \ln\left(\frac{C_0}{C}\right).$$

where k is the release rate constant; t is the release time; C_0 is the initial concentration; and C is the current concentration.

3. Results and Discussion

3.1. Characterization of Calcite Microparticles

The X-ray diffraction method was utilized for studying $CaCO_3$ microparticles synthesized by the method of an ion exchange reaction of salts according to reaction 1. According to Fig. 3, it was established that the reflexes and their intensities for the obtained microparticles corresponded to the literature data for calcite (23° (1906), 30° (13800), 36° (2100), 39° (2960), 44° (2700), 47° 2500), 49° (2600)), which confirms the formation of the desired polymorphic modification of $CaCO_3$ – calcite.[53–55]

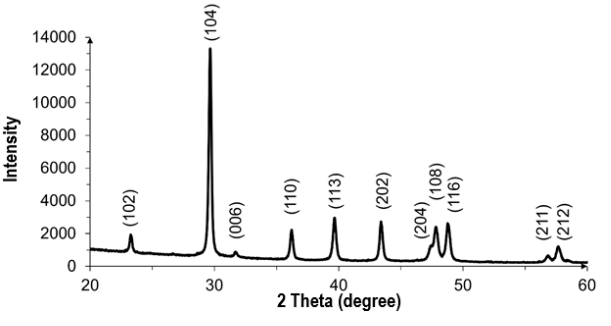

Fig. 3. Diffraction pattern of the synthesized calcite microparticles

Transmission electron microscopy (TEM) combined with energy dispersive spectroscopy was utilized to

confirm the chemical purity of the synthesized $CaCO_3$ microparticles and determine the content of atoms of each type (Table 1).

The EDX analysis detected calcium, oxygen, copper, and magnesium in the structure of microparticles. The presence of Mg can be caused by impurities in the calcium chloride used for the synthesis of microparticles. The presence of Cu can be a consequence of copper mesh utilization during the EDX analysis.

The morphology of the synthesized $CaCO_3$ particles was analyzed using transmission electron microscopy. As can be seen from Fig. 4, ellipsoid calcite microparticles are characterized by an average size of 1.5×2.0 μm.

Table 1. EDX analysis of synthesized $CaCO_3$ microparticles

Element	Content, wt %	Content, mole %
Calcium (Ca)	62.2 ± 0.4	42.1 ± 0.4
Oxygen (O)	32.8 ± 0.5	55.6 ± 0.5
Copper (Cu)	4.8 ± 0.2	2.0 ± 0.2
Magnesium (Mg)	0.2 ± 0.02	0.19 ± 0.02

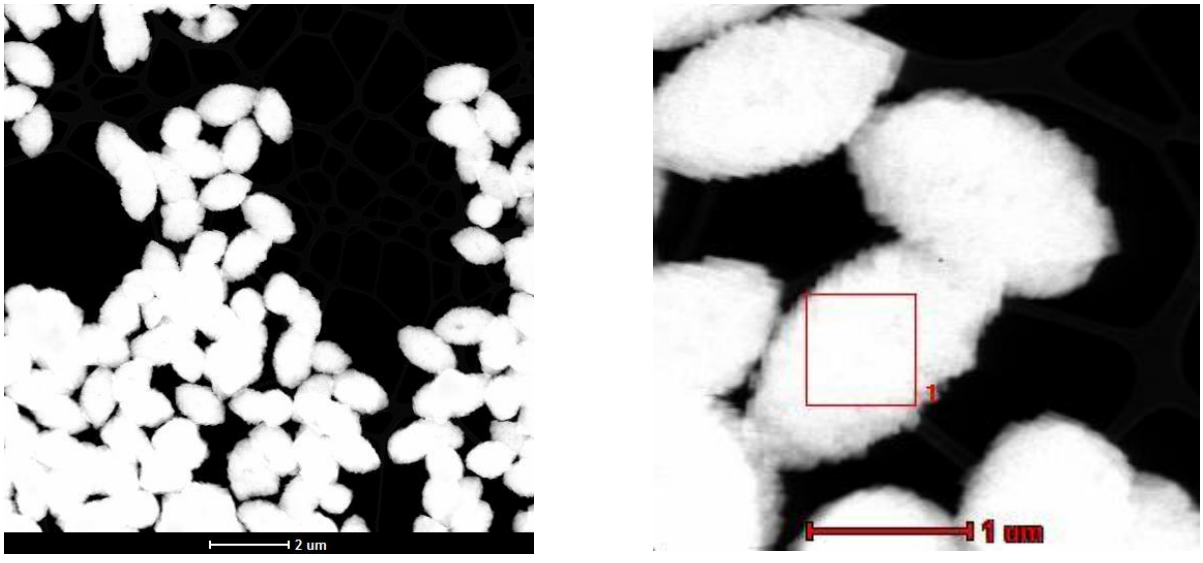

a) b)

Fig. 4. TEM images of $CaCO_3$ microparticles with magnification: a) 2 μm; b) 1 μm

The adsorption of ethonium on the surface of microparticles of calcium carbonate was determined to confirm the sorption of ethonium on the surface of $CaCO_3$ microparticles[56,57] in the process of sample preparation. It was established that the limit value of ethonium adsorption on synthesized microparticles of calcium carbonate was 1.47 mg of ethonium per 1 mg of $CaCO_3$.

3.2. Characterization of Ca-Alg and Ca-AlgM

Crosslinking of polysaccharide chains using Ca^{2+} ions occurred according to the reaction illustrated in Fig. 2. Ca^{2+} ions were formed *in situ* during $CaCO_3$ MPs decomposition by hydrochloric acid (reaction 2). As a result, the macropores (diameter > 50 nm)[58,59] appeared at the location of calcite microparticles.

The presence of macropores on the samples' surface can be assumed based on a visual assessment of the surface microphotographs acquired by scanning electron microscopy. According to the measuring scale of the device: the average range of diameters of the pores is 50–140 nm for Ca-Alg (Fig. 5a) and 50–150 nm for Ca-AlgM (Fig. 5b).

Swelling degrees were evaluated by the gravimetric method at different pH values. Regardless of the pH value Ca-Alg (Fig. 6a) and Ca-AlgM (Fig. 6b) reached an equilibrium state after 40 and 60 min, respectively. According to the results, the hydrogels demonstrated high swelling indexes (α >150%[60,61]). Moreover, the swelling degree did not change during further immersion in an aqueous environment. Ca-AlgM was characterized by a higher swelling ratio compared to Ca-Alg regardless of the medium pH which can be explained by a higher surface area and volume of micropores formed during the crosslinking process.

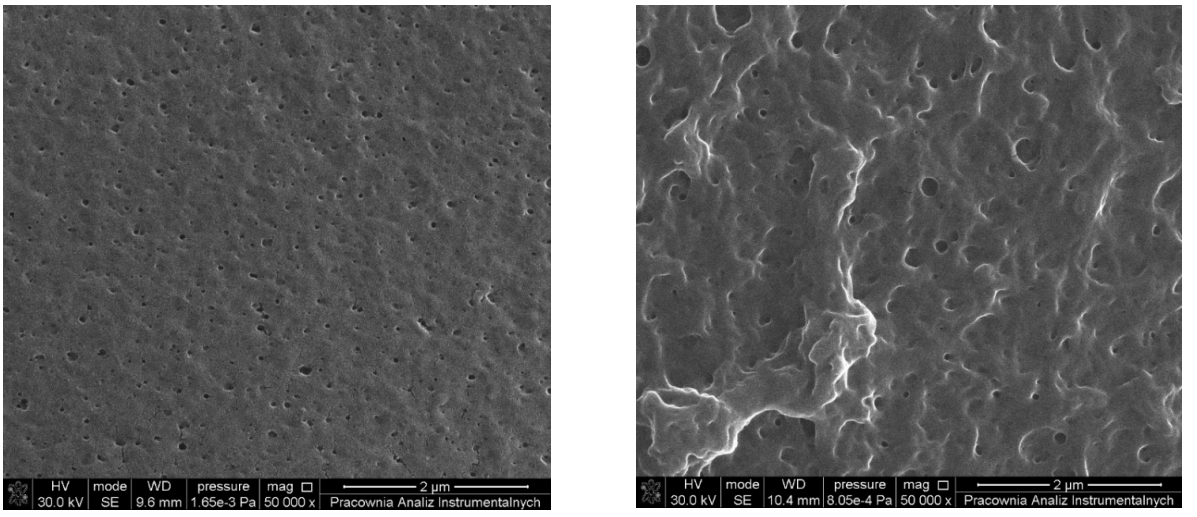

a) b)

Fig. 5. SEM images of a) Ca-Alg, b) Ca-AlgM films

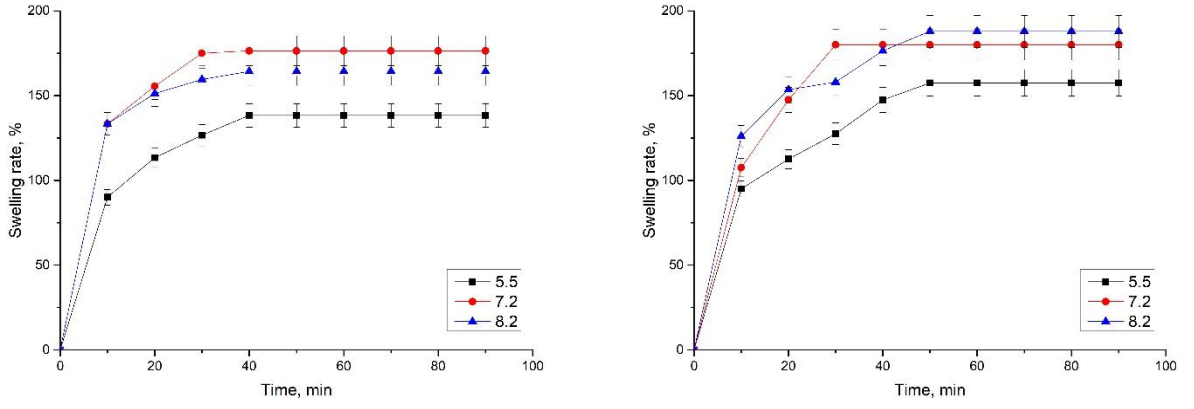

a) b)

Fig. 6. Kinetics of swelling at different pH values for a) Ca-Alg and b) Ca-AlgM at $t = 20$ °C

The pH-sensitivity of swelling was more observable for Ca-Alg: the lowest degree of swelling was characteristic of a solution with a pH value of 5.5, and the highest one for a neutral medium with a pH of 7.2. The same tendency, namely, a lower swelling degree in an acidic medium and a higher swelling degree in a neutral medium, was noticed for Ca-AlgM.

3.3. Characterization of Ca-Alg+Eth and Ca-AlgM+Eth

Ca-Alg and Ca-AlgM films with immobilized ethonium were fabricated by adding ethonium to NaAlg + $CaCO_3$ and NaAlgM + $CaCO_3$ forming solutions with subsequent crosslinking using a hydrochloric acid. The presence and characteristics of mesopores (diameter from 2 to 50 nm)[58,59] in the samples were investigated by the method of nitrogen adsorption and desorption. The hysteresis loops for the Ca-Alg+Eth and Ca-AlgM+Eth samples (Fig. 7.) differed from each other, which indicates differences in the size and number of pores in the samples. In particular, the larger volume of adsorbate absorbed by the sample based on NaAlgM indicates a larger volume of micropores compared to NaAlg, which was confirmed by data calculated based on isotherms (Table 2).

The increase of surface area and volume of micropores for Ca-AlgM+Eth compared to Ca-Alg+Eth was achieved due to the formation of a higher number of pores because of AlgM cross-linking characteristics. AlgM has modified carboxyl groups that cannot form bonds with Ca^{2+}.[50] That leads to the formation of a more compact and ordered hydrogel structure with reduced size of pores compared to Ca-Alg+Eth due to the formation of hydrophobic-hydrophobic interactions between ethonium and AlgM carbon chains.

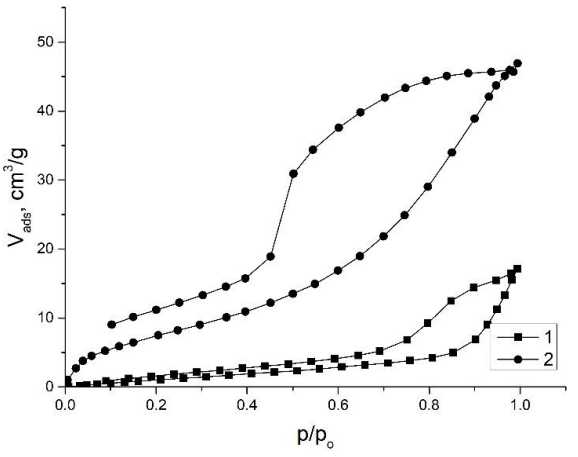

Fig. 7. Adsorption and desorption isotherms for 1) Ca-Alg+Eth; 2) Ca-AlgM+Eth

Table 2. Summarized results investigated by the nitrogen adsorption-desorption method

Sample	Surface area, m^2/g	Volume of micropores $\cdot 10^3$, cm^3/g	Average pore size, nm
Ca-Alg+Eth	7.0	26.7 ± 0.5	5.5 ± 0.5
Ca-AlgM+Eth	30.0	72.7 ± 0.5	2.7 ± 0.5

The size distribution of pores for Ca-Alg+Eth and Ca-AlgM+Eth is presented in Fig. 8. According to the obtained data, each sample has only one type of micropore with a low size range. These results are consistent with the proposed method of pore formation due to the simultaneous release of CO_2 bubbles during crosslinking of the samples according to reaction 2.

The kinetics of the release of immobilized ethonium from the hydrogel films was evaluated at different pH values because the developed samples can be used for transdermal systems of controlled drug delivery. Each sample was examined 3 times and the statistical error of the results did not exceed 5%. It was confirmed that the samples showed partial pH sensitivity of release at a temperature of 20°C (Fig. 9), which disappeared with an increase in temperature to 37°C (Fig. 10). The minimal pH sensitivity of the release kinetics was a consequence of the insignificant pH sensitivity of the swelling of Ca-Alg and Ca-AlgM samples at 20°C (Fig. 6). The reason for the disappearance of the pH sensitivity of the release with increasing temperature is ethonium immobilization. In the process of sample preparation, ethonium was sorbed on the surface of calcium carbonate microparticles.[56,57] As a result, during the decomposition of calcite, ethonium was concentrated in the pores formed in the crosslinking process; thus, ethonium is released from pores during the swelling process according to the laws of diffusion.[62]

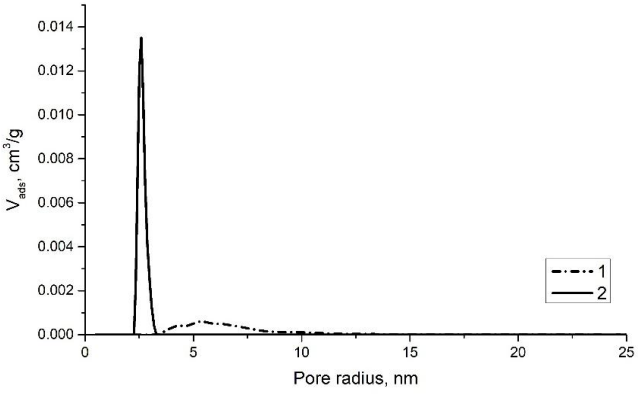

Fig. 8. The size distribution of mesopores investigated by the adsorption-desorption method for 1) Ca-Alg+Eth; 2) Ca-AlgM+Eth

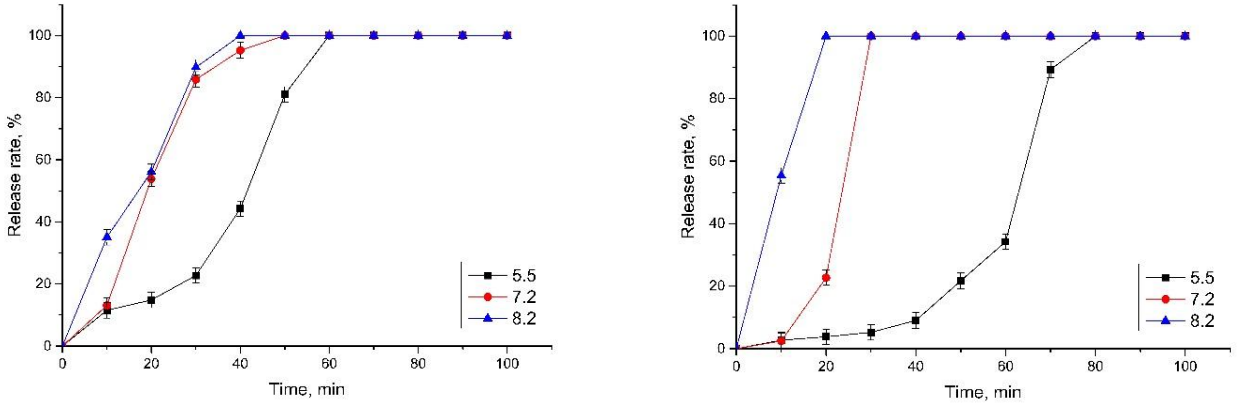

a) b)

Fig. 9. Kinetics of ethonium release from a) Ca-Alg-Eth; b) Ca-AlgM-Eth at t = 20°C

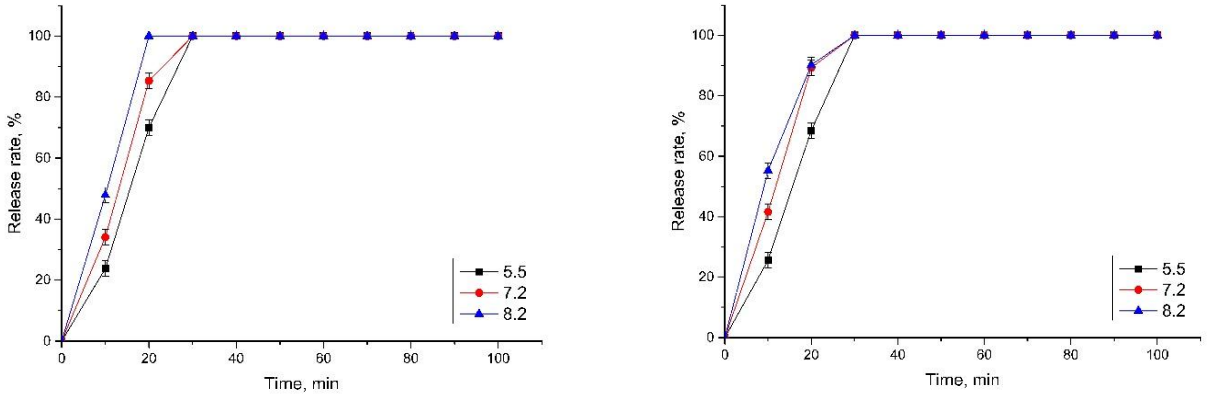

Fig. 10. Kinetics of ethonium release from a) Ca-Alg-Eth; b) Ca-AlgM-Eth at t = 37 °C

The constants of ethonium release were calculated to confirm the differences in the ethonium release process from the Ca-Alg-Eth and Ca-AlgM-Eth compared to the films prepared without calcite microparticles:[50] 1.2–9.6 · 10^{-3} min^{-1} for non-calcite samples compared to 40.8–109.8 · 10^{-3} min^{-1} (Table 3). Such differences indicate that the most conceivable reason for such differences is the effect of ethonium adsorption on $CaCO_3$ microparticles during the formation of hydrogels.[63,64]

Table 3. Constants of drug release from investigated samples

Sample	pH	T°C	$k \cdot 10^3$, min^{-1}
Ca-Alg+Eth	5.5	20	40 ± 1
		37	72 ± 1
	7.2	20	94 ± 1
		37	108 ± 1
	8.2	20	95 ± 1
		37	109 ± 1
Ca-AlgM+Eth	5.5	20	57 ± 1
		37	68 ± 1
	7.2	20	76 ± 1
		37	108 ± 1
	8.2	20	77 ± 1
		37	110 ± 1

To summarize, the proposed crosslinking method allows for immediate drug release, as a consequence the bioavailability of active substances increases and the time of onset of the therapeutic effect reduces.

4. Conclusions

Samples of alginate films based on sodium alginate and alginate modified with octan-1-amine were fabricated using microparticles of calcium carbonate and immobilized ethonium. Calcite microparticles were synthesized by the method of coprecipitation of salts and characterized by an oval shape with an average particle size of 1.5×2.0 μm. The authenticity and purity of the obtained particles were confirmed by the methods of transmission electron microscopy and X-ray diffraction. The kinetics of swelling of alginate films cross-linked with Ca^{2+} ions formed *in situ* by decomposition of $CaCO_3$ microparticles using hydrochloric acid was studied. The significant pH sensitivity of swelling at 20ºC was not revealed. The scanning electron microscopy demonstrated the formation of pores on the surface of the samples with average diameters of 50-140 nm for Ca-Alg and 50-150 nm for Ca-AlgM.

Hydrogel films with immobilized ethonium were investigated using the nitrogen adsorption-desorption method, and the presence of mesopores with an average radius of 2.7 ± 0.5 and 5.5 ± 0.5 for Ca-Alg+Eth and Ca-AlgM+Eth, respectively, was established. The kinetics of ethonium release at different temperatures and pH were evaluated. The obtained results of the study of the immobilized drug release indicate the same effectiveness of using the original and modified alginate. The results of the release kinetics of the immobilized drug indicate the same effectiveness for using the original and modified alginate: in 30 minutes at physiological temperature, the immobilized drug is completely released regardless of pH. This fact opens prospects for the development of drug delivery systems not only for external but also for internal use with immediate release based on a cheap natural polysaccharide.

The proposed fabrication method of polymeric porous hydrogel films allows the development of transdermal systems for targeted drug delivery. Such systems in the form of adhesive plasters can provide not only mechanical protection of wounds from contamination but also maintain the moisture of the bottom of open wounds, which will reduce the drying out of nerve endings and relieve pain. The findings of this study may have significant implications for medical and scientific research.

Acknowledgements

This work was supported by a grant from the Simons Foundation, Proposal ID: 1290592 (2024) and by the Ukraine Future Leadership Program, which is administered by the Institute of International Education and made possible by the Freeman Foundation.

References

[1] Xue, H.; Ju, Y.; Ye, X.; Dai, M.; Tang, C.; Liu, L. Construction of Intelligent Drug Delivery System Based on Polysaccharide-Derived Polymer Micelles: A Review. *Int. J. Biol. Macromol.* **2024**, *254*, 128048. https://doi.org/10.1016/j.ijbiomac.2023.128048
[2] Galasso, C.; Ruocco, N.; Mutalipassi, M.; Barra, L.; Costa, V.; Giommi, C.; Dinoi, A.; Genovese, M.; Pica, D.; Romano, C.; Greco, S.; Pennesi, C. Marine Polysaccharides, Proteins, Lipids, and Silica for Drug Delivery Systems: A Review. *Int. J. Biol. Macromol.* **2023**, *253*, 127145. https://doi.org/10.1016/j.ijbiomac.2023.127145
[3] Putro, J. N.; Soetaredjo, F. E.; Lunardi, V. B.; Irawaty, W.; Yuliana, M.; Santoso, S. P.; Puspitasari, N.; Wenten, I. G.; Ismadji, S. Polysaccharides Gums in Drug Delivery Systems: A Review. *Int. J. Biol. Macromol.* **2023**, *253*, 127020. https://doi.org/10.1016/j.ijbiomac.2023.127020
[4] Gomzyak, V. I.; Sedush, N. G.; Puchkov, A. A.; Polyakov, D. K.; Chvalun, S. N. Linear and Branched Lactide Polymers for Targeted Drug Delivery Systems. *Polym. Sci. Ser. B* **2021**, *63*, 257–271. https://doi.org/10.1134/S1560090421030064
[5] Elumalai, K.; Srinivasan, S.; Shanmugam, A. Review of the Efficacy of Nanoparticle-Based Drug Delivery Systems for Cancer Treatment. *Biom. Techn.* **2024**, *5*, 109–122. https://doi.org/10.1016/j.bmt.2023.09.001
[6] Wen, H.; Jung, H.; Li, X. Drug Delivery Approaches in Addressing Clinical Pharmacology-Related Issues: Opportunities and Challenges. *AAPS J.* **2015**, *17*, 1327–1340. https://doi.org/10.1208/s12248-015-9814-9
[7] Raina, N.; Pahwa, R.; Bhattacharya, J.; Paul, A. K.; Nissapatorn, V.; Pereira, M. de L.; Oliveira, S. M. R.; Dolma, K. G.; Rahmatullah, M.; Wilairatana, P. *et al*. Drug Delivery Strategies and Biomedical Significance of Hydrogels: Translational Considerations. *Pharmaceutics* **2022**, *14*, 1–31. https://doi.org/10.3390/pharmaceutics14030574
[8] Hussain, M.; Hafeez, A.; Kushwaha, S. P. Nanoformulation Mediated Transdermal Delivery of Anti-Diabetic Drugs: An Updated Review. *Intell. Pharm.* **2023**, *1*, 192–200. https://doi.org/10.1016/j.ipha.2023.08.009
[9] Xu, Y.; Zhao, M.; Cao, J.; Fang, T.; Zhang, J.; Zhen, Y.; Wu, F.; Yu, X.; Liu, Y.; Li, J.; *et al*. Applications and Recent Advances in Transdermal Drug Delivery Systems for the Treatment of Rheumatoid Arthritis. *Acta Pharm. Sin. B* **2023**, *13*, 4417–4441. https://doi.org/10.1016/j.apsb.2023.05.025
[10] Parihar, A.; Prajapati, B. G.; Paliwal, H.; Shukla, M.; Khunt, D.; Devrao Bahadure, S.; Dyawanapelly, S.; Junnuthula, V. Advanced Pulmonary Drug Delivery Formulations for the Treatment of Cystic Fibrosis. *Drug Discov. Today* **2023**, *28*, 103729. https://doi.org/10.1016/j.drudis.2023.103729
[11] Xiong, S.; Ye, S.; Ni, P.; Zhong, M.; Shan, J.; Yuan, T.; Liang, J.; Fan, Y.; Zhang, X. Polyvinyl-Alcohol, Chitosan and Graphene-Oxide Composed Conductive Hydrogel for Electrically Controlled Fluorescein Sodium Transdermal Release. *Carbohydr. Polym.* **2023**, *319*, 121172. https://doi.org/10.1016/j.carbpol.2023.121172
[12] Vasowala, T.; Gharat, S.; Mhase, M.; Momin, M. Advances in Hydrogels Based Cutaneous Drug Delivery System for Management of Psoriasis. *Eur. Polym. J.* **2024**, *202*, 112630. https://doi.org/10.1016/j.eurpolymj.2023.112630
[13] Schoenmakers, D. C.; Rowan, A. E.; Kouwer, P. H. J. Crosslinking of Fibrous Hydrogels. *Nat. Commun.* **2018**, *9*, 1–8. https://doi.org/10.1038/s41467-018-04508-x
[14] Peppas, N. A.; Hilt, J. Z.; Khademhosseini, A.; Langer, R. Hydrogels in Biology and Medicine: From Molecular Principles to Bionanotechnology. *Adv. Mater.* **2006**, *18*, 1345–1360. https://doi.org/10.1002/adma.200501612
[15] Varaprasad, K.; Raghavendra, G. M.; Jayaramudu, T.; Yallapu, M. M.; Sadiku, R. A Mini Review on Hydrogels Classification and Recent Developments in Miscellaneous Applications. *Mater. Sci. Eng. C* **2017**, *79*, 958–971. https://doi.org/10.1016/j.msec.2017.05.096
[16] Alven, S.; Aderibigbe, B. A. Chitosan and Cellulose-Based Hydrogels for Wound Management. *Int. J. Mol. Sci.* **2020**, *21*, 1–30. https://doi.org/10.3390/ijms21249656
[17] Dreiss, C. A. Hydrogel Design Strategies for Drug Delivery. *Curr. Opin. Colloid Interface Sci.* **2020**, *48*, 1–17. https://doi.org/10.1016/j.cocis.2020.02.001
[18] Chang, S. H.; Custer, P. L.; Mohadjer, Y.; Scott, E. Use of Lorenz Titanium Implants in Orbital Fracture Repair. *Ophthal. Plast. Reconstr. Surg.* **2009**, *25*, 119–122. https://doi.org/10.1097/IOP.0b013e31819ac7c5
[19] Wang, L.; Neumann, M.; Fu, T.; Li, W.; Cheng, X.; Su, B. L. Porous and Responsive Hydrogels for Cell Therapy. *Curr. Opin. Colloid Interface Sci.* **2018**, *38*, 135–157. https://doi.org/10.1016/j.cocis.2018.10.010
[20] El-Sherbiny, I. M.; Yacoub, M. H. Hydrogel Scaffolds for Tissue Engineering: Progress and Challenges. *Glob. Cardiol. Sci. Pract.* **2013**, *2013*, 38. https://doi.org/10.5339/gcsp.2013.38
[21] Tiwari, R.; Pathak, K. Local Drug Delivery Strategies towards Wound Healing. *Pharmaceutics* **2023**, *15*, 1–39. https://doi.org/10.3390/pharmaceutics15020634
[22] Zhao, X.; Wu, H.; Guo, B.; Dong, R.; Qiu, Y.; Ma, P. X. Antibacterial Anti-Oxidant Electroactive Injectable Hydrogel as Self-Healing Wound Dressing with Hemostasis and Adhesiveness for Cutaneous Wound Healing. *Biomaterials* **2017**, *122*, 34–47. https://doi.org/10.1016/j.biomaterials.2017.01.011
[23] Harrison, I. P.; Spada, F. Hydrogels for Atopic Dermatitis and Wound Management: A Superior Drug Delivery Vehicle. *Pharmaceutics* **2018**, *10*, 71. https://doi.org/10.3390/pharmaceutics10020071
[24] Affes, S.; Aranaz, I.; Acosta, N.; Heras, Á.; Nasri, M.; Maalej, H. Chitosan Derivatives-Based Films as pH-Sensitive Drug Delivery Systems with Enhanced Antioxidant and Antibacterial Properties. *Int. J. Biol. Macromol.* **2021**, *182*, 730–742. https://doi.org/10.1016/j.ijbiomac.2021.04.014

[25] Sarwar, M. S.; Ghaffar, A.; Huang, Q.; Zafar, M. S.; Usman, M.; Latif, M. Controlled-Release Behavior of Ciprofloxacin from a Biocompatible Polymeric System Based on Sodium Alginate/Poly(Ethylene Glycol) Mono Methyl Ether. *Int. J. Biol. Macromol.* **2020**, *165*, 1047–1054. https://doi.org/10.1016/j.ijbiomac.2020.09.196
[26] Aliakbar Ahovan, Z.; Esmaeili, Z.; Eftekhari, B. S.; Khosravimelal, S.; Alehosseini, M.; Orive, G.; Dolatshahi-Pirouz, A.; Pal Singh Chauhan, N.; Janmey, P. A.; Hashemi, A. *et al*. Antibacterial Smart Hydrogels: New Hope for Infectious Wound Management. *Mater. Today Bio* **2022**, *17*, 100499. https://doi.org/10.1016/j.mtbio.2022.100499
[27] Khan, S.; Ullah, A.; Ullah, K.; Rehman, N. U. Insight into Hydrogels. *Des. Monomers Polym.* **2016**, *19*, 456–478. https://doi.org/10.1080/15685551.2016.1169380
[28] Chai, Q.; Jiao, Y.; Yu, X. Hydrogels for Biomedical Applications: Their Characteristics and the Mechanisms behind Them. *Gels* **2017**, *3*, 6. https://doi.org/10.3390/gels3010006
[29] Catoira, M. C.; Fusaro, L.; Di Francesco, D.; Ramella, M.; Boccafoschi, F. Overview of Natural Hydrogels for Regenerative Medicine Applications. *J. Mater. Sci. Mater. Med.* **2019**, *30*, 115. https://doi.org/10.1007/s10856-019-6318-7
[30] Tavakoli, S.; Klar, A. S. Advanced Hydrogels as Wound Dressings. *Biomolecules* **2020**, *10*, 1–20. https://doi.org/10.3390/biom10081169
[31] Bashir, S.; Hina, M.; Iqbal, J.; Rajpar, A. H.; Mujtaba, M. A.; Alghamdi, N. A.; Wageh, S.; Ramesh, K.; Ramesh, S. Fundamental Concepts of Hydrogels: Synthesis, Properties, and Their Applications. *Polymers (Basel)* **2020**, *12*, 1–60. https://doi.org/10.3390/polym12112702
[32] Banerjee, R.; Kumar, K. J.; Kennedy, J. F. Structure and Drug Delivery Relationship of Acidic Polysaccharides: A Review. *Int. J. Biol. Macromol.* **2023**, *243*, 125092. https://doi.org/10.1016/j.ijbiomac.2023.125092
[33] Hurtado, A.; Aljabali, A. A. A.; Mishra, V.; Tambuwala, M. M.; Serrano-Aroca, Á. Alginate: Enhancement Strategies for Advanced Applications. *Int. J. Mol. Sci.* **2022**, *23*, 4486. https://doi.org/10.3390/ijms23094486
[34] Maiti, S.; Maji, B.; Yadav, H. Progress on Green Crosslinking of Polysaccharide Hydrogels for Drug Delivery and Tissue Engineering Applications. *Carbohydr. Polym.* **2023**, *326*, 121584. https://doi.org/10.1016/j.carbpol.2023.121584
[35] Xie, Y.; Kollampally, S. C. R.; Jorgensen, M.; Zhang, X. Alginate Microfibers as Therapeutic Delivery Scaffolds and Tissue Mimics. *Exp. Biol. Med.* **2022**, *247*, 2103–2118. https://doi.org/10.1177/15353702221112905
[36] Cao, Y., Cong, H., Yu, B., Shen, Y. A Review on the Synthesis and Development of Alginate Hydrogels for Wound Therapy. *J. Mater. Chem. B* **2023**, *11*, 2801–2829. https://doi.org/10.1039/d2tb02808e
[37] Wang, C.; Liu, H.; Gao, Q.; Liu, X.; Tong, Z. Alginate-Calcium Carbonate Porous Microparticle Hybrid Hydrogels with Versatile Drug Loading Capabilities and Variable Mechanical Strengths. *Carbohydr. Polym.* **2008**, *71*, 476–480. https://doi.org/10.1016/j.carbpol.2007.06.018
[38] Robertsa, J.R.; Rittera, D. W.; McShane, M.J. A Design Full of Holes: Functional Nanofilm-Coated Microdomains in Alginate Hydrogels. *J Mater Chem B Mater Biol Med.* **2013**, *107*, 3195–3201. https://doi.org/10.1039/C3TB20477D
[39] Zhou, Z.; Zhou, S.; Zhang, X.; Zeng, S.; Xu, Y.; Nie, W.; Zhou, Y.; Xu, T.; Chen, P. Quaternary Ammonium Salts: Insights into Synthesis and New Directions in Antibacterial Applications. *Bioconjug. Chem.* **2023**, *34*, 302–325. https://doi.org/10.1021/acs.bioconjchem.2c00598
[40] Obłąk, E.; Piecuch, A.; Rewak-Soroczyńska, J.; Paluch, E. Activity of Gemini Quaternary Ammonium Salts against Microorganisms. *Appl. Microbiol. Biotechnol*. **2019**, *103*, 625–632. https://doi.org/10.1007/s00253-018-9523-2
[41] Tischer, M.; Pradel, G.; Ohlsen, K.; Holzgrabe, U. Quaternary Ammonium Salts and Their Antimicrobial Potential: Targets or Nonspecific Interactions? *Chem.Med.Chem* **2012**, *7*, 22–31. https://doi.org/10.1002/cmdc.201100404
[42] Hoque, J.; Akkapeddi, P.; Yarlagadda, V.; Uppu, D. S. S. M.; Kumar, P.; Haldar, J. Cleavable Cationic Antibacterial Amphiphiles: Synthesis, Mechanism of Action, and Cytotoxicities. *Langmuir* **2012**, *28*, 12225–12234. https://doi.org/10.1021/la302303d
[43] Xue, Y.; Xiao, H.; Zhang, Y. Antimicrobial Polymeric Materials with Quaternary Ammonium and Phosphonium Salts. *Int. J. Mol. Sci*. **2015**, *16*, 3626–3655. https://doi.org/10.3390/ijms16023626
[44] Ivantsyk, L. B.; Drogovoz, S. M.; Gerbina, N. A.; Kalĸo, K. A.; Shtroblia, V. V. Advantages of the Composition and Actyvity of a New Combined Ointment with Ethony for Treatment of the Wound Process. *Likarska Sprava* **2019**, *2019*, 126–133. https://doi.org/10.31640/jvd.1-2.2019(19)
[45] Obłak, E.; Piecuch, A.; Krasowska, A.; Łuczyński, J. Antifungal Activity of Gemini Quaternary Ammonium Salts. *Microbiol. Res.* **2013**, *168*, 630–638. https://doi.org/10.1016/j.micres.2013.06.001
[46] Guo, R.; Du, X.; Zhang, R.; Deng, L.; Dong, A.; Zhang, J. Bioadhesive Film Formed from a Novel Organic-Inorganic Hybrid Gel for Transdermal Drug Delivery System. *Eur. J. Pharm. Biopharm.* **2011**, *79*, 574–583. https://doi.org/10.1016/j.ejpb.2011.06.006
[47] Prausnitz, M. R.; Langer, R. Transdermal Drug Delivery. *Nat. Biotechnol.* **2008**, *26*, 1261–1268. https://doi.org/10.1038/nbt.1504
[48] Li, N.; Qin, Y.; Dai, D.; Wang, P.; Shi, M.; Gao, J.; Yang, J.; Xiao, W.; Song, P.; Xu, R. Transdermal Delivery of Therapeutic Compounds With Nanotechnological Approaches in Psoriasis. *Front. Bioeng. Biotechnol.* **2022**, *9*, 804415. https://doi.org/10.3389/fbioe.2021.804415
[49] Goncharuk, O.; Gunko, V. M.; Ugnivenko, A.; Terpilowski, K.; Skwarek, E.; Janusz, W. Effect of Ethonium Adsorption on Structure Formation in Nanosilica Dispersions. *Nano Res. Appl.* **2017**, *03*, 1–7. https://doi.org/10.21767/2471-9838.100029
[50] Sikach, A. V.; Konovalova, V. V.; Kolesnyk, I. S. Hydrogel Films Based on Sodium Alginate Modified With Octane-1-Amine: Enhanced Pore Formation and Potential Applications in Drug Delivery Systems. *Khimia, Fizyka ta Tehnologia Poverhni* **2024**, *15*, 43–56. https://doi.org/10.15407/hftp15.01.043
[51] Kumar, P.; Honnegowda, T. Effect of Limited Access Dressing on Surface pH of Chronic Wounds. *Plast. Aesthetic Res.* **2015**, *2*, 257. https://doi.org/10.4103/2347-9264.165449
[52] Ainurofiq, A.; Choiri, S. Model and Release Pattern of Water Soluble Drug from Natural-Polymer Based Sustained Release Tablet Dosage Form. *Int. J. Pharm. Pharm. Sci.* **2014**, *6*, 179–182.
[53] Li, L.; Yang, Y.; Lv, Y.; Yin, P.; Lei, T. Porous Calcite $CaCO_3$ Microspheres: Preparation, Characterization and Release Behavior as Doxorubicin Carrier. *Colloid Surfaces B.* **2020**, *186*, 110720. https://doi.org/10.1016/j.colsurfb.2019.110720
[54] Kumar, A. S.; Prema, D.; Rao, R. G.; Prakash, J.; Balashanmugam, P.; Devasena, T.; Venkatasubbu, G. D. Fabrication of Poly (Lactic-Co-Glycolic Acid)/Gelatin Electro Spun Nanofiber Patch

Containing $CaCO_3/SiO_2$ Nanocomposite and Quercetin for Accelerated Diabetic Wound Healing. *Int. J. Biol. Macromol.* **2024**, *254*, 128060. https://doi.org/10.1016/j.ijbiomac.2023.128060
[55] Nirmala Devi, M.; Sanjiv Raj, K.; Subramanian, V. K. Synergistic Effects of Magnesium and EDTA on Polymorphism and Morphology of $CaCO_3$ and Its Influence on Scale. *J. Cryst. Growth* **2021**, *564*, 126108. https://doi.org/10.1016/j.jcrysgro.2021.126108
[56] Boyjoo, Y.; Pareek, V. K.; Liu, J. Synthesis of Micro and Nano-Sized Calcium Carbonate Particles and Their Applications. *J. Mater. Chem. A* **2014**, *2*, 14270–14288. https://doi.org/10.1039/c4ta02070g
[57] Meng, L.; Wang, J.; Liu, Q.; Fan, Z. Hydrophobic Calcium Carbonate with Hierarchical Micro-/Nanostructure for Improving Foaming Capacity. *Mater. Res. Express* **2019**, *6*, 1250c8. https://doi.org/10.1088/2053-1591/ab63fc
[58] Sing, K. S. W. Reporting Physisorption Data for Gas/Solid Systems. *Pure Appl. Chem.* **1982**, *54*, 2201–2218. https://doi.org/10.1351/pac198254112201
[59] Ma, X.; Du, Y.; Fu, C.; Fang, H.; Wei, H.; Pan, Z.; Sang, S.; Zhang, J. Effects of Supercritical CO_2 on the Pore Structure Complexity of High-Rank Coal with Water Participation and the Implications for CO2ECBM. *ACS Omega* **2023**, *8*, 18964–18980. https://doi.org/10.1021/acsomega.3c01486
[60] Chen, J.; Nichols, B. L. B.; Norris, A. M.; Frazier, C. E.; Edgar, K. J. All-Polysaccharide, Self-Healing Injectable Hydrogels Based on Chitosan and Oxidized Hydroxypropyl Polysaccharides. *Biomacromolecules* **2020**, *21*, 4261–4272. https://doi.org/10.1021/acs.biomac.0c01046
[61] Feng, W.; Wang, Z. Tailoring the Swelling-Shrinkable Behavior of Hydrogels for Biomedical Applications. *Adv. Sci.* **2023**, *10*, 1–41. https://doi.org/10.1002/advs.202303326
[62] Longsworth, L. G. Temperature Dependence of Diffusion in Aqueous Solutions. *J. Phys. Chem.* **1954**, *58*, 770–773. https://doi.org/10.1021/j150519a017
[63] Farzan, M.; Roth, R.; Schoelkopf, J.; Huwyler, J.; Puchkov, M. The Processes behind Drug Loading and Release in Porous Drug Delivery Systems. *Eur. J. Pharm. Biopharm.* **2023**, *189*, 133–151. https://doi.org/10.1016/j.ejpb.2023.05.019
[64] Frenning, G. Modelling Drug Release from Inert Matrix Systems: From Moving-Boundary to Continuous-Field Descriptions. *Int. J. Pharm.* **2011**, *418*, 88–99. https://doi.org/10.1016/j.ijpharm.2010.11.030

Received: February 21, 2024 / Revised: May 14, 2024 / Accepted: June 11, 2024

ПОРИСТІ ГІДРОГЕЛЕВІ ПЛІВКИ НА ОСНОВІ НАТРІЙ АЛЬГІНАТУ ЯК НОСІЇ ДЛЯ СИСТЕМ ІМПУЛЬСНОЇ ДОСТАВКИ ЛІКІВ

Анотація. *Це дослідження зосереджено на створенні методу виробництва іонно-зшитих гідрогелевих систем на основі альгінату, які забезпечують негайне вивільнення ліків. Дослідження вивчає кінетику вивільнення бактерицидного препарату для полегшення процесу загоєння. Методика передбачає покращення методу іммобілізації амфіфільних лікарських засобів на мікрочастинках кальциту з наступним їхнім концентруванням у порах, утворених унаслідок розкладання мікрочастинок.*

Ключові слова: *альгінатні гідрогелі, полісахаридні плівки, мікрочастинки кальцій карбонату, система доставки ліків, етоній, іонне зшивання.*